Desiccating Stress-Induced MMP Production and Activity Worsens Wound Healing in Alkali-Burned Corneas

Fang Bian, Flavia S. A. Pelegrino, Stephen C. Pflugfelder, Eugene A. Volpe, De-Quan Li, and Cintia S. de Paiva

Ocular Surface Center, Department of Ophthalmology, Cullen Eye Institute, Baylor College of Medicine, Houston, Texas, United States

Correspondence: Cintia S. de Paiva, Cullen Eye Institute, Baylor College of Medicine, 6565 Fannin Street, NC 505G, Houston, TX 77030, USA; cintiadp@bcm.edu.

Submitted: February 6, 2015
Accepted: June 12, 2015

Citation: Bian F, Pelegrino FSA, Pflugfelder SC, Volpe EA, Li D-Q, de Paiva CS. Desiccating stress-induced MMP production and activity worsens wound healing in alkali-burned corneas. *Invest Ophthalmol Vis Sci*. 2015;56:4908–4918. DOI:10.1167/iovs.15-16631

Purpose. To evaluate the effects of dry eye on ocular surface protease activity and sight threatening corneal complications following ocular surface chemical injury.

Methods. C57BL/6 mice were subjected to unilateral alkali burn (AB) with or without concomitant dry eye for 2 or 5 days. Mice were observed daily for appearance of corneal perforation. Whole corneas were harvested and lysed for RNA extraction. Quantitative real-time PCR was performed to measure expression of inflammation cytokines, matrix metalloproteinases (MMP). Matrix metalloproteinase–9 activity, gelatinase activity, and myeloperoxidase (MPO) activity were evaluated in corneal lysates. Presence of infiltrating neutrophils was evaluated by immunohistochemistry and flow cytometry.

Results. Eyes subjected to the combined model of AB and dry eye (CM) had 20% sterile corneal perforation rate as soon as 1 day after the initial injury, which increased to 35% by 5 days, delayed wound closure and increased corneal opacity. Increased levels of IL-1β, -6, and MMPs-1, -3, -8, -9, and -13, and chemokine (C-X-C motif) ligand 1 (CSCL1) transcripts were found after 2 days in CM compared with AB corneas. Increased MMP-1, -3, -9, and -13 immunoreactivity and gelatinolytic activity were seen in CM corneas compared with AB. Increased neutrophil infiltration and MPO activity was noted in the CM group compared with AB 2 days post injury.

Conclusions. Desiccating stress worsens outcome of ocular AB, creating a cytokine and protease storm with greater neutrophil infiltration, increasing the risk of corneal perforation.

Keywords: alkali injury, dry eye, neutrophils, MMPs, ocular perforation

Eye injuries in the military and civilian population are frequent events.[1–4] The main causes of eye injuries in the military has changed with changes in strategy and weaponry. These include sharp, blast fragmentation, penetrating, and perforating injuries of the globe, occasionally with intraocular foreign bodies to ocular surface chemical, thermal, nuclear, and laser burns.[5,6] Sulfur mustard gas can potentially cause severe ocular surface injury, including blepharospasm, lid edema, and corneal ulceration. This chemical warfare agent has been in several military conflicts, including the recent Iran–Iraq War.[7,8]

Barely detected in an unwounded cornea, matrix metalloproteinases (MMPs) are strongly induced during wound healing and chemical burns. The MMP family includes more than 25 members that can be divided into collagenases (MMPs-1, -8, and -13, that degrades collagen types I, II, and III); gelatinases (MMP-2 and -9 that degrade collagen types IV, V, VII, and X as well as decorin, fibronectin, and laminin); stromelysins (MMP-3 and -10); matrilysins (MMP-7 and -26 that degrade proteoglycans, laminin, and glycoproteins substrates); and the membrane-type MMPs that are bound to epithelial cell membranes, and can activate MMPs, according to their structure and substrate specificity (MMP-14 to -17 and -24).[9–12] Collectively, these MMPs are able to degrade the entire extracellular matrix and basement membranes components.

Both chemical and thermal injuries to the surface of the eye have a high potential to cause blindness. These injuries often damage the epithelium covering the cornea, conjunctiva, and eyelid margins and in more severe cases destroy the stem cells that renew these epithelia. In many cases, the supporting stromal cells and matrix are damaged and chronic inflammation is induced. Furthermore, most patients with severe ocular surface injuries develop a secondary dry eye due to destruction of tear producing cells, which has the potential to worsen the outcome. In addition to lubricating the ocular surface, the tears contain numerous growth and anti-inflammatory factors that are essential for wound repair and suppressing inflammation and tissue destruction.

The controlled desiccating environment many of us live in is under recognized as an initiator of dry eye–induced ocular surface inflammation. Virtually all modern office buildings are air-conditioned, often with high flow, low humidity air. Low humidity (in offices, aircraft cabins, deserts, and winter season) impacts tear film and ocular health.[13] While it is currently known that low humidity exposure increases tear evaporation rate and increases frequency of eye irritation,[14,15] specific inflammatory pathways/mediators that are stimulated are poorly understood.

The purpose of this study was to study the effects of dry eye on ocular surface protease activity following corneal chemical injury. A combined model of alkali burn (AB) and dry eye was

used to evaluate the effects of experimental dry eye on inflammatory cytokines, chemokines, and MMPs (-1, -2, -3, -8, -9, -12, and -13) after ocular surface chemical injury and the consequences of increase protease activity on corneal epithelial healing.

Materials and Methods

Animals

This research protocol was approved by the Baylor College of Medicine Center for Comparative Medicine (Houston, TX, USA), and it conformed to the standards in the ARVO Statement for the use of Animals in Ophthalmic and Vision Research.

Unilateral Alkali Burn

After systemic anesthesia with isoflurane using a vaporizer (SomnoSuite; Kent Scientific, Torrington, CT, USA), a unilateral AB was created on the right eye of 6- to 8-week-old C57BL/6 mice. This was achieved by placing one 2-mm diameter filter paper disc that had been presoaked with 1N NaOH on the central cornea for 10 seconds, followed by extensive rinsing with balanced salt solution (Alcon, Fort Worth, TX, USA), as previously described.[16] Precautions were taken to avoid damage to the peripheral cornea, conjunctiva, and lids. Alkali burn was created at day 0 and animals were euthanized after 2 or 5 days. A separate group of animals (n = 6) were followed for up to 21 days. The contralateral eyes served as untreated (UT) controls. A separate group of mice that received unilateral AB were also subjected to desiccating stress (DS) after anesthetic recovery for 2 or 5 days (AB+DS, referred to as the combined model = CM). The contralateral eyes served as desiccating stress controls (not AB, but in a low humidity environment).

Desiccating stress was induced in female C57BL/6 mice aged 6 to 8 weeks by sterile subcutaneous injection of 0.5 mg/1 mL scopolamine hydrobromide (Sigma-Aldrich Corp., St. Louis, MO, USA) quater in die (QID) into alternating flanks and exposure to a drafty low humidity (<30% relative humidity) environment for 2 or 5 days (DS, DS2, and DS5, respectively) as previously described.[17] Mice subjected to AB or CM received no eyedrops or antibiotics.

At least 45 animals without corneal perforations were used per group (AB and CM) and per time point: 12 for histology (6 for frozen sections and 6 for paraffin), 12 for corneal opacity and wound closure, 15 for real-time PCR, 4 for myeloperoxidase assay, 4 for MMP-9 assay, and 10 for flow cytometry. Corneal opacity and wound closure rate were evaluated in 12 live mice that were used for either histology, PCR, or flow cytometry. Contralateral eyes in the AB group were used as untreated controls; while contralateral eyes in CM group were used as DS controls. Whenever an ocular perforation was observed, mice were euthanized, and removed from the study with the exception of the histology as shown in Figure 1.

Clinical Findings: Ocular Perforation and Opacity Score

All eyes in each treatment group were examined daily under a microscope (SMZ 1500; Nikon, Melville, NY, USA) for the presence of any corneal perforation. Once corneal perforation was observed, mice were euthanized. Perforated corneas were not used for any experiments other than the histology. The number of corneal perforations occurring each day was recorded and survival curves were calculated using Graph Pad Prism 6.0 software (GraphPad Software, Inc., San Diego, CA, USA).

Corneal edema and opacity were graded by two masked observers in images taken with a microscope equipped with a color digital camera (DS-Fi1; Nikon) by the method described by Yoeruek.[18] Corneal opacity was scored using a grading scale of 0 to 4: grade 0 = completely clear; grade 1 = slightly hazy, iris and pupils easily visible; grade 2 = slightly opaque, iris and pupils still detectable; grade 3 = opaque, pupils hardly detectable, and grade 4 = completely opaque with no view of the pupils.

Measurement of Corneal Epithelial Defect

Corneal epithelial healing was assessed daily in the experimental groups (four individual right corneas/group/experiment; three sets of experiments). Briefly, 1 μL 0.1% liquid sodium fluorescein was instilled onto the ocular surface. Corneas were rinsed with PBS and photographed with a stereoscopic zoom microscope (SMZ 1500; Nikon) under fluorescence excitation at 470 nm (DS-Qi1Mc; Nikon). Corneal epithelial defects were graded in digital images by two masked observers in a categorical manner (present/absent) to generate a survival curve. Biological replicate scores were transferred to excel database where the results were analyzed.

Ocular Cultures

Cornea and conjunctiva of mice that developed corneal perforations were swabbed using sterile cotton swabs and plated on sheep blood agar and transported to the microbiology laboratory at the Methodist Hospital (Houston, TX, USA) for routine bacterial and fungal cultures to identify any potential microbial infection as cause for the corneal perforation. Culture plates were read each day for the first 2 days and then again at the seventh day after seeding.

Histology and Immunostaining

Mice were euthanized either 2 or 5 days after initial injury. Eyes and adnexae (n = 6/experimental group/time point) were surgically excised, fixed in 10% formalin, paraffin embedded, and 8-μm tissue sections were cut. These sections were stained with hematoxylin and eosin (H&E) for evaluating morphology and inflammatory signs. They were examined and photographed with a microscope equipped with a digital camera (Eclipse E400 with a DS-Fi1; Nikon).

For immunohistochemistry, additional eyes and adnexae from each group/time point (n = 6/experimental group/time point) were excised, embedded in optimal cutting temperature compound (VWR, Suwanee, GA, USA), and flash frozen in liquid nitrogen. Sagittal 8-μm tissue sections were cut with a cryostat (HM 500; Micron, Waldorf, Germany) and placed on glass slides that were stored at −80°C. Immunohistochemistry was performed to detect neutrophils using rat anti-Gr-1 antibody (Ly6G, 1:250, clone 1A8; BD Pharmingen, San Diego, CA, USA). Cryosections were stained with the primary antibody and appropriate biotinylated secondary antibody (1:100 biotin goat anti-rat; BD Pharmingen) using a Vectastain Elite ABC kit and Nova Red reagent (Vector, Burlingame, CA, USA). Six sections from each animal/group/time point were examined and photographed with microscope equipped with a digital camera (Eclipse E400 with a DS-Qi1Mc; Nikon). The numbers of Gr-1 positive (+) cells were counted in cornea sections from each animal at ×20 magnification and results were averaged and expressed as the number of positive cells per cornea.

Immunofluorescent staining for IL-1β and MMPs was performed in frozen tissue sections with rabbit polyclonal antibody anti–MMP-1 (1:50, NBP1-77209; Novus Biologicals, (Littleton, CO, USA), anti–MMP-9 (1:100 dilution; Santa Cruz Biotechnology, Dallas, TX, USA), anti–IL-1β (1:100; Upstate-Millipore Corp., Bedford, MA, USA), and goat anti–MMP-3 and

Investigative Ophthalmology & Visual Science

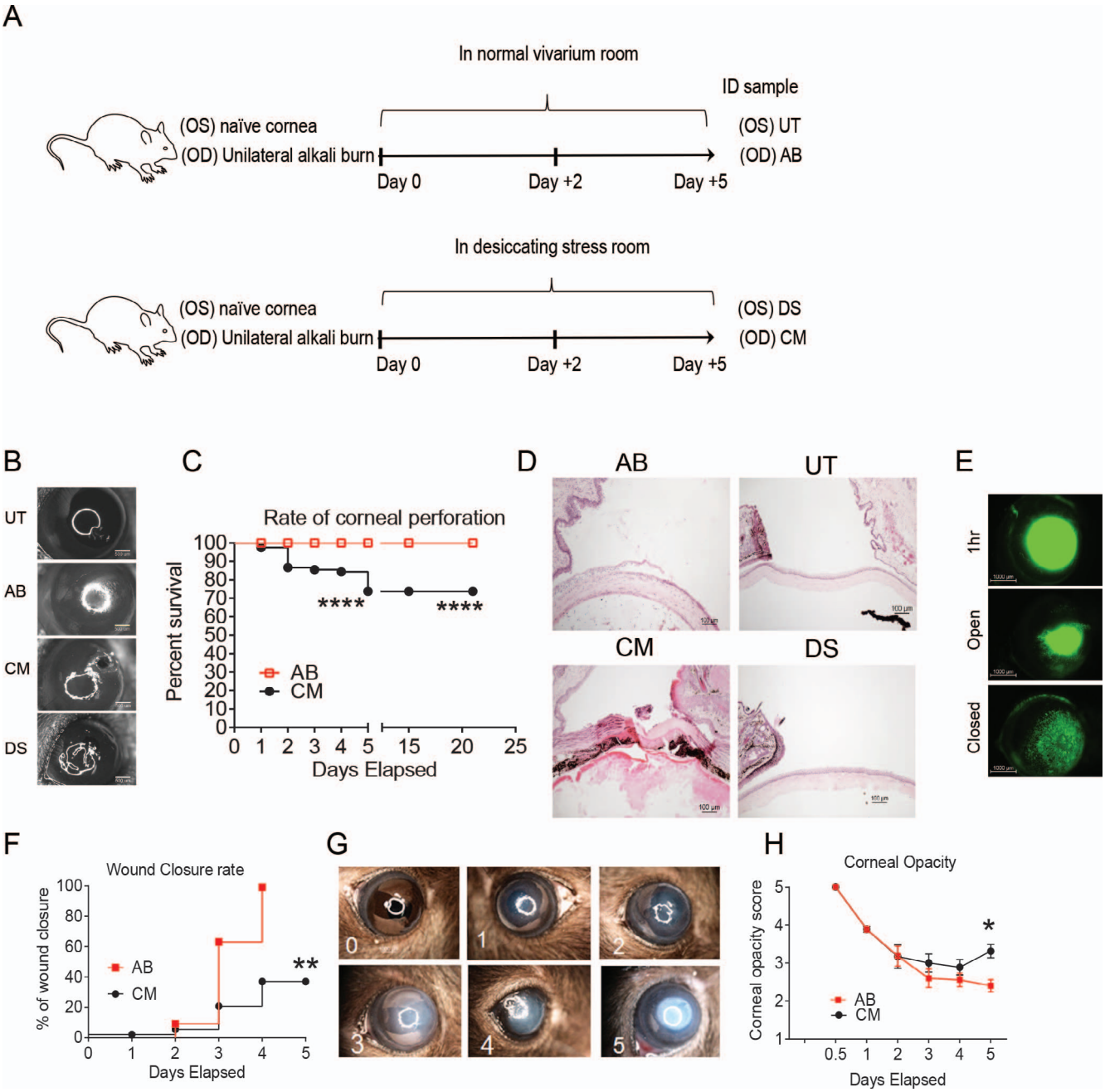

Figure 1. Dry eye jeopardized cornea integrity after AB injury. **(A)** Schematic of experimental design. A unilateral AB in the right cornea was performed as described in the Materials and Methods. Mice were then kept in a normal vivarium room (resulting in AB and UT corneas) or subjected to DS in a specially designed room (resulting in DS or combined model [CM = AB + DS] corneas). **(B)** Digital images of bright field pictures from control, AB, CM, and DS 5 days post injury. Note: perforation in the combined group. **(C)** Rate of ocular perforation in eyes subjected to AB and CM. **(D)** Representative H&E staining of cryosections from control, AB, CM, and 5 days post injury. Perforated CM corneas developed massive inflammatory infiltration forming waves of inflammatory cells within the cornea stroma. Cornea perforation is sealed by lens and iris. Alkali-burned corneas had loose epithelium and moderate inflammatory cells in the cornea stroma and anterior chamber. Original magnification: ×10. **(E)** Representative digital images of corneas 1 hour after creation of AB lesion and representative pictures of open and closed wounds 2 and 5 days after initial lesion used to generate the survival curve of corneal re-epithelization seen in **(F)**. **(F)** Survival rate of wound closure in AB and CM groups. **(G)** Representative bright field digital images of corneas showing opacification scale used to generate the graph seen in ([**H**]; corneal opacity score). **(H)** Corneal opacity score in AB and CM groups. $^{*}P < 0.05$; $^{**}P < 0.01$; $^{****}P < 0.0001$.

anti–MMP-13 (1:100, SC6839 and SC-123630, respectively, both from Santa Cruz Biotechnology). Secondary goat-anti rabbit or donkey anti-goat Alexa-Fluor 488 conjugated IgG antibodies were used, as previously described.[19] The images were captured and photographed by a Nikon fluorescence microscope (Eclipse E400 equipped with a DS–F1 digital camera).

RNA Isolation and Quantitative PCR

Five whole corneas/group/time point/per experiment (total of three independent experiments) were excised, minced, and total RNA was extracted using a Qiagen MicroPlus RNeasy isolation Kit (Qiagen, Valencia, CA, USA) according to the

Table. Taqman Probes Used for Real-Time PCR

Gene Name	Symbol	Assay ID*
Interleukin 1 alpha	*IL1-α*	Mm00439620
Interleukin 1 beta	*IL1-β*	Mm00434228
Interleukin 6	*IL-6*	Mm99999064
Chemokine (C-X-C motif) ligand 1	*CXCL1*	Mm04207460
Matrix metalloproteinase 1	*MMP-1*	Mm00473493
Matrix metalloproteinase 2	*MMP-2*	Mm00439506
Matrix metalloproteinase 3	*MMP-3*	Mm00440295
Matrix metalloproteinase 8	*MMP-8*	Mm00439509
Matrix metalloproteinase 9	*MMP-9*	Mm00442991
Matrix metalloproteinase 12	*MMP-12*	Mm00500554
Matrix metalloproteinase 13	*MMP-13*	Mm00439491
Hypoxanthine guanine phosphoribosyl transferase 1	*Hprt-1*	Mm00446968

* Identification number from Life Technologies (in the public domain, www.lifetechnologies.com).

manufacturer's instructions, quantified by a NanoDrop ND-2000 Spectrophotometer (Thermo Scientific, Wilmington, DE, USA) and stored at −80°C. First-strand cDNA was synthesized with random hexamers by M-MuLV reverse transcription (Ready-To-Go You-Prime First-Strand Beads; GE Healthcare, Inc., Arlington Heights, NJ, USA), as previously described.[20]

Real-time PCR was performed with specific Taqman minor groove binder (MGB) probes (Applied Biosystems, Inc., Foster City, CA, USA) and PCR master mix (Taqman Gene Expression Master Mix), in a commercial thermocycling system (StepOnePlus Real-Time PCR System; Applied Biosystems), according to the manufacturer's recommendations. Quantitative real-time PCR was performed using gene expression assay primers and MGB probes specific for murine targets as described in the Table. The hypoxanthine guanine phosphoribosyl transferase (*HPRT-1*) gene was used as an endogenous reference for each reaction to correct for differences in the amount of total RNA added. The results of quantitative PCR were analyzed by the comparative cycle threshold (C_T) method where target change $= 2^{-}(\triangle)(\triangle)^{C}{}_{T}$. The results were normalized by the C_T value of HPRT-1 and the relative mRNA level in the untreated group was used as the calibrator.

Myeloperoxidase Assay

Myeloperoxidase (MPO) activity was measured using a myeloperoxidase colorimetric activity assay kit as described by the manufacturer (Sigma-Aldrich Corp.). Briefly, whole-cornea lysates from AB, CM, or control corneas ($n = 4$ samples/group/time point) were homogenized in MPO assay buffer and the homogenate was centrifuged at 14,000*g* for 20 minutes at 4°C. Total protein concentration was measured by the BCA protein assay as previously described.[17] A 50 μg/sample was mixed with MPO assay buffer and MPO substrate, incubated at room temperature for 2 hours, and then mixed with tetramethylbenzidine probe. Fluorescence was measured at 412 nm using a Tecan Infinite M200 plate reader (Tecan, Inc., San Jose, CA, USA) equipped with Magellan V6.55 software (Tecan, Inc.). Biological replicate samples were averaged. Results are presented as mean ± SEM (milliunits).

MMP-9 Activity Assay

Whole corneas were excised, rinsed, and homogenized in RIPA buffer and the homogenate was centrifuged at 14,000*g* for 20 minutes at 4°C. Total protein concentration of the whole-cornea cell lysate ($n = 4$/group/time point) was measured by the BCA protein assay as previously described.[17] Total MMP-9 enzyme activity was measured with a MMP activity assay kit (Biotrak; Amersham Biosciences, Piscataway, NJ, USA) according to the manufacturer's protocol as previously published.[21] In brief, 100 μL each pro–MMP-9 standard (0.125–4 ng/mL), 50 μg cornea extract and assay buffer (for blanks) were incubated at 4°C overnight in wells of a microtiter plate precoated with anti–mouse-MMP-9 antibodies and washed. Total MMP-9 activity was measured by activating bound pro–MMP-9 with 50 μL 0.5 mM p-amino phenylmercuric acetate (APMA) in assay buffer at 37°C for 1.5 hours, followed by incubation with a detection reagent at 37°C for 2 hours. Active MMP-9 was detected through its ability to activate a modified prodetection enzyme that subsequently cleaved to its chromogenic peptide substrate. Absorbance was read at 405 nm using a Tecan Infinite M200 plate reader equipped with Magellan V6.55 software. The activity of MMP-9 in a sample was determined by interpolation from a standard curve. Biological replicates were averaged and the results were presented as mean ± SEM (pg/mL).

Gelatin Zymography

The relative amount of MMP-9 in whole-cornea lysates ($n = 4$/group) was measured by gelatin zymography, using a previously reported method.[22,23] Whole-cornea lysates prepared for MMP-9 activity (20 μg/sample) were fractionated in an 8% polyacrylamide gel containing gelatin (0.5 mg/mL). The gels were soaked in 0.25% Triton X-100 for 30 minutes at room temperature, then incubated in a digestion buffer containing 5 mM phenylmethyl sulfonyl fluoride at 37°C overnight. They were stained with 0.25% Coomassie brilliant blue R-250 in 40% methanol for 2 hours, then destained overnight in 10% acetic acid. Gelatinolytic activities appeared as clear bands of digested gelatin against a dark blue background of stained gelatin.

Flow-Cytometry Analysis of Infiltrating Cells in Cornea

Single-cell suspensions of corneas ($n = 5$/group/time point/experiment, for a total of two experiments) were excised, rinsed, and prepared by treatment of minced tissue fragments with 0.1% collagenase D (60 minutes at 37°C; Invitrogen-Gibco, Carlsbad, CA, USA) and sequentially neutralized with media and filtered, then resuspended and stained with anti-CD16/32 (BD Pharmingen), followed by cell-surface staining with FITC-F4/80 (clone BM8; Biolegend, San Diego, CA, USA), PE-Gr-1 (clone 1A8; BD Pharmingen), and APC-CD45 (clone 30-F11; BD Pharmingen). Single-cell preparations of bone marrow cells obtained from control mice were stained with the same antibodies and served as positive controls. Cells were kept on ice until flow cytometry analysis was performed. A BD LSRII Benchtop cytometer was used. The gating strategy was as follows: lymphocytes were individually identified on the basis of forward scatter and side scatter properties, subsequently gated on the basis of forward scatter height versus forward scatter area (singlets 1), then gated on side scatter height versus side scatter area (singlets 2), followed by CD45 histogram gating. Propidium iodide exclusion was used to discriminate live cells. At least 50,000 events were collected. Results were analyzed with BD Diva software (version 2.1; BD Pharmingen) and FlowJo software (version 10.07; Tree Star, Inc., Ashland, OR, USA).

Statistical Analysis

Results are presented as the mean ± SEM. Two-way ANOVA with Bonferroni post hoc testing was used for statistical comparisons of gene expression. *P* less than or equal to 0.05

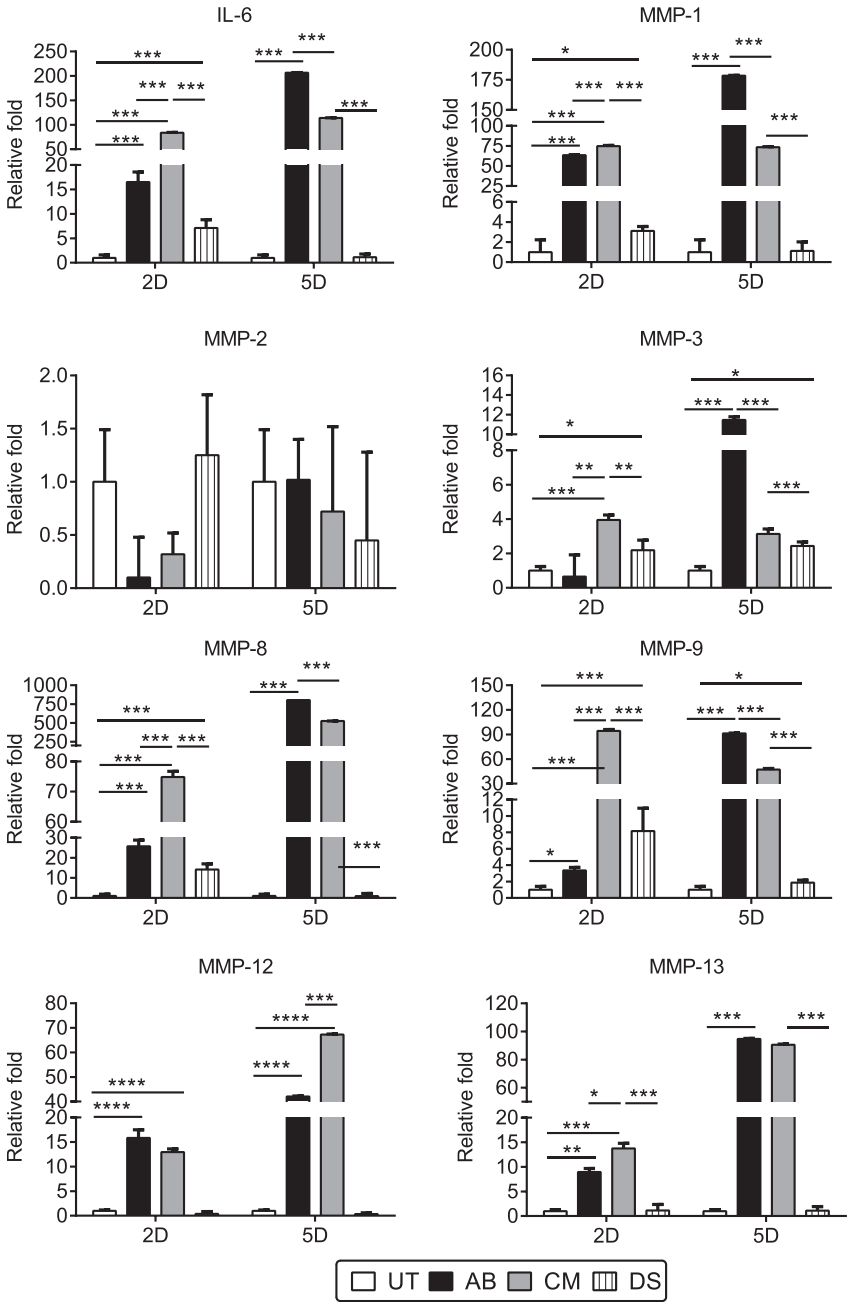

Figure 2. Early increase cytokine and MMP storm in combined model corneas. Relative fold of expression of IL-6 and MMPs-1, -2, -3, -8, -9, -12, and -13, in whole corneas subjected to AB or CM. *Bar graphs* show means ± SEM of one representative experiment with five samples per group/time point (experiment was repeated thrice with similar results). $^{*}P < 0.05$, $^{**}P < 0.01$, $^{***}P < 0.001$, $^{****}P < 0.0001$.

was considered statistical significant. These tests were performed using GraphPad Prism 6.0 software.

Results

Concomitant Alkali Burn and Desiccating Stress Leads to Ocular Perforation

Because environmental dry eye is an under recognized variable in the management of severe burned patients, including the ones treated in intensive care units, we have developed a CM of AB and dry eye by subjecting mice to desiccating stress immediately after anesthetic recovery following creation of AB (Fig. 1A). We observed that eyes subjected to CM perforated as early as 2 days post initial injury (20%) and the rate of perforation in some experiments was up to 40% by day 5 (Figs. 1B, 1C), while eyes subjected to AB alone did not perforate. Naïve and DS corneas did not perforate at all (data not shown). Corneas that did not perforate in the initial 5 days post injury did not perforate at later time point (even up to 21 days), showing that the initial inflammatory has the greatest effect on corneal integrity (Fig. 1C). Histologically, perforated corneas subjected to the CM had collapsed anterior chamber, iris, and lens tamponade, total loss of corneal epithelium and massive infiltration of corneal stroma by inflammatory cells that dissected into the cornea from the limbus (Fig. 1D). Microbial cultures of perforated corneas and conjunctivas ($n = 6$)

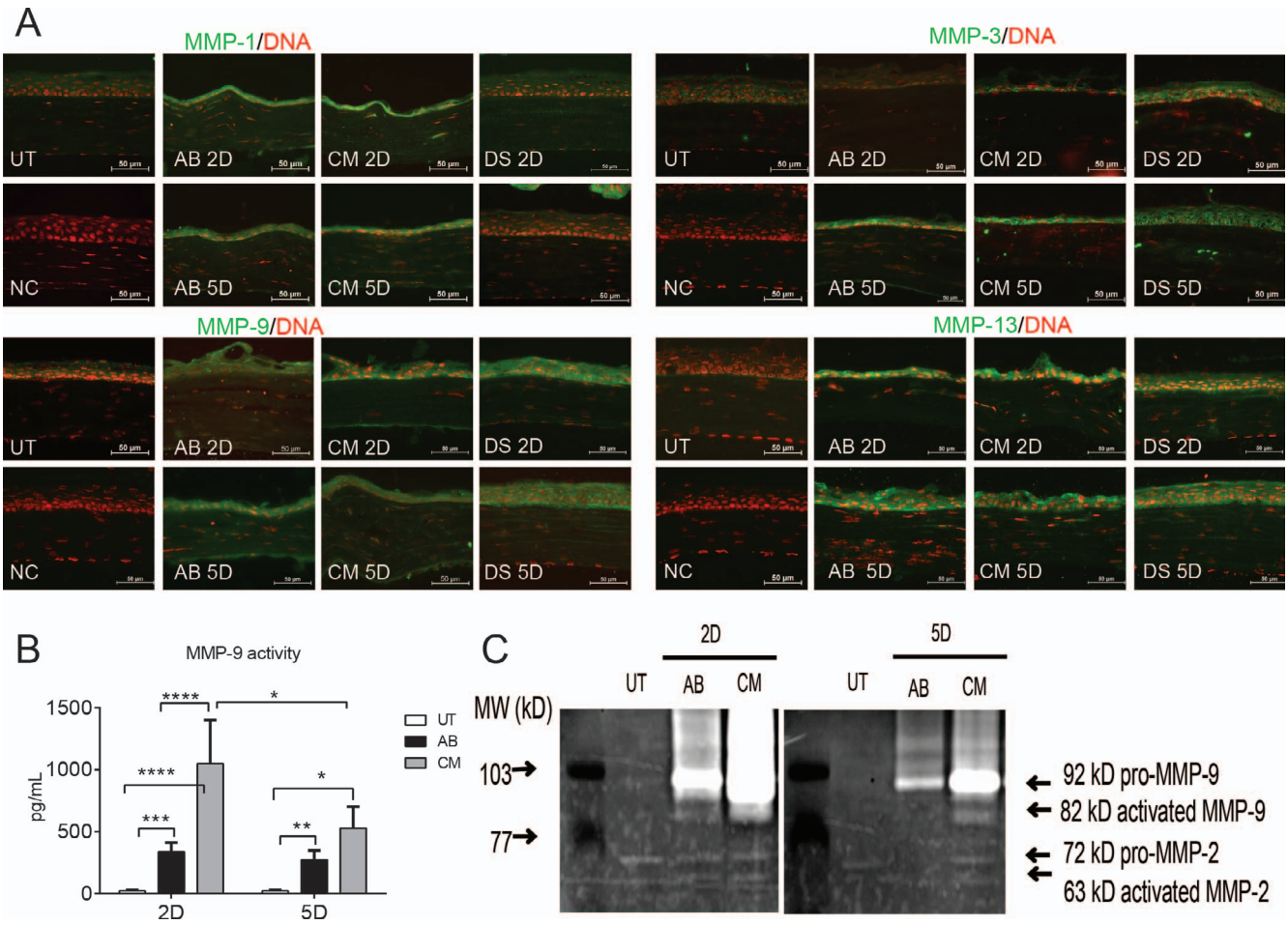

Figure 3. Increased MMP protein expression in combined model of AB and dry eye. (**A**) Representative merged digital images of corneas cryosections immunostained for MMP-1, -3, -13, and -9 (all in *green*) with propidium iodide nuclei counterstaining (*red*) in corneas subjected to AB, DS, or CM. *Scale bars*: 50 μm. (**B**) Matrix metalloproteinase–9 activity in whole-cornea lysates in AB, CM, and untreated group. (**C**) Representative zymogram showing MMP-9 bands whole-cornea lysates in the treatment groups. $^{*}P < 0.05$, $^{**}P < 0.01$, $^{***}P < 0.001$, $^{****}P < 0.0001$.

showed no microorganism growth, confirming the sterile nature of the perforation. Eyes subjected to AB had a central corneal epithelial defect and moderate inflammatory infiltration in the corneal stroma, but no perforation.

We evaluated wound closure by staining corneas with 0.1% fluorescein daily and generated a survival curve of wound closure based on presence/absence of epithelial wound closure, independent of the area left to be closed (Figs. 1E, 1F). The CM corneas had delayed re-epithelization compared to AB alone (40% vs. 100% by day 5, respectively, Fig. 1E). We also graded daily corneal opacification in digital images captured daily by masked examiners using a scale from 0 (transparent cornea) to 5 (complete opaque cornea, Fig. 1G). We observed higher residual cornea opacification in the CM group compared with corneas subjected to AB alone (Fig. 1H).

Taken together, these results show that combining dry eye with AB induces sterile corneal perforation in in up to 40% of the cases, delays wound healing and increases corneal opacity.

Cytokine and MMPs Storm in the Combined Model

It has been recognized for decades that ocular surface chemical/thermal injury stimulates production of tissue degrading enzymes as part of the wound healing cascade.[16,22,24–26] Matrix degrading enzymes, including MMPs have been identified as important factors in the inflammatory and wound healing response of the ocular surface, particularly in dry eye and ocular burns. Their induction during wound healing is thought to play a role in extracellular matrix remodeling, cytokine activation, and regulation of angiogenesis.

Because most of cornea perforations and greatest differences in cornea wound healing were seen early (at 2 and 5 days post injury), we evaluated the levels of RNA transcripts encoding IL-1α, IL-6, and MMPs-1, -2, -3, -8, -9, -12, and -13, by real-time PCR using whole corneas harvested from all groups at these same time points. Our results are presented in Figure 2.

Two days post injury, both AB and CM groups had significantly elevated expression of IL-6 and MMPs compared with untreated corneas; however, CM significantly increased IL-6 (83- vs. 17-fold), MMP-1 (75- vs. 63-fold), MMP-3 (4- vs. 0.7-fold), MMP-8 (75- vs. 26-fold), MMP-9 (95- vs. 4-fold), MMP-13 (14- vs. 9-fold) mRNA transcripts compared with AB alone. Desiccating stress corneas had upregulation of IL-6, MMPs-1, -3, -8, and -9 compared with naïve corneas, however, this increase was significantly lower than the one observed in the AB and CM corneas. Five days post injury, AB corneas had significantly elevated IL-6 and MMPs-1, -3, -8, and -9, mRNA transcripts compared with the CM group (Fig. 2). Interleukin-1α was equally elevated in both CM and AB groups after 2 and 5 days post injury (2.7- vs. 1.7-fold and 2.5- vs. 3-fold, respectively)

compared with control corneas (data not shown). Desiccating stress corneas had significantly elevated expression of MMP-3 and -9 after 5 days of desiccating stress, as we previously reported.[17,19,27]

Matrix metalloproteinase–12, also known as macrophage elastase, and produced by macrophages, fibroblasts, and epithelial cells[28–31] was equally elevated in both AB and CM corneas 2 days after injury (15.85 ± 1.66– vs. 12.97 ± 0.65–fold) but at 5 days its expression significantly increased in the CM group (42.03 ± 0.23– vs. 67.30 ± 0.18–fold, $P < 0.001$).

The immunoreactivity of corneas to collagenases (MMP-1 and -13[32]), MMP-3 (a physiological activator of MMP-9[33]), and -9 were evaluated by immunostaining (Fig. 3A). Minimal staining of MMPs-1, -3, -9, and -13 was noted in the control corneas, while increased immunoreactivity was observed in the corneal epithelium of CM, AB, and DS corneas (DS < AB < CM).

Among the MMPs, MMP-9 plays a prominent role being produced by stressed cornea and conjunctival epithelial cells and has both matrix degrading and proinflammatory activities.[34–36] Matrix metalloproteinase–9 have been reported to delay corneal wound healing.[37] We evaluated MMP-9 activity in whole-cornea lysates using an MMP-9 activity assay and observed that the CM group had significantly higher levels of active MMP-9 than AB both at day 2 and day 5 post injury (Fig. 3B). Gelatin zymography showed increased amounts of both pro and active MMP-9 bands in the CM and AB groups compared with control corneas (Fig. 3C); however, as suspected from the MMP-9 activity assay, greater amounts of pro and activated MMP-9 bands were present in the CM group. Negligible amounts of MMP-2 were present in AB and CM groups and they did not differ from untreated corneas.

These results indicated that the early peak of inflammatory cytokines and MMPs in the CM group coincides with the time period where most of the corneal perforations occur, indicating that the early additive effect of dry eye with AB jeopardizes corneal integrity.

Increased Infiltration of Neutrophils in the CM Group

Polymorphonuclear leukocytes (neutrophils) are the first inflammatory cells to migrate into sites of tissue injury. The pathogenic role of neutrophils in AB can be appreciated as neutrophil-depleted C57BL/6 corneas subjected to AB healed faster than nondepleted controls.[38]

Interleukin-1 is a cytokine produced by epithelium, fibroblasts, and neutrophils[39,40] and participates in collagen degradation by stimulating neutrophils.[41] The chemokine chemokine (C-X-C motif) ligand 1 (CXCL1) is crucial for the recruitment of neutrophils to inflammatory sites.[42] We evaluated expression of IL-1β and CXCL1 in corneas subjected to AB and CM and compared with controls. The CM significantly increased IL-1β (72- vs. 11-fold) and CXCL1 (27- vs. 5-fold) 2 days after injury compared with AB alone. At 5 days, IL-1β levels maintained elevated in CM (393- vs. 267-fold) and similar levels of CXCL1 were seen 5 days post injury in both models (~20-fold; Fig. 4A). Minimal expression of IL-1β was seen in untreated corneas; however, AB and CM increased immunoreactivity in corneal epithelium to IL-1β, which peaked at day 5 post injury.

We evaluated presence of neutrophils in injured corneas by immunohistochemistry using the Gr-1 marker, flow cytometry and also by myeloperoxidase activity assay in whole-cornea lysates. In a naïve cornea, a few resident neutrophils can be found at the limbal area (data not shown). A significant influx of Gr-1$^+$ cells was observed in AB and CM groups 2 and 5 days post injury; the infiltration was not restricted to the limbal area (Fig. 4B, inset), but extended to the central cornea (Fig. 4B). The CM corneas had the highest Gr-1$^+$ cell counts (Fig. 4C) compared with AB and UT corneas 2 days after injury. These results were confirmed by flow cytometry as we observed a significant increase in CD45$^+$ cells in corneas subjected to AB and CM (Fig. 4D); the majority of CD45$^+$ infiltrating cells were Gr-1$^+$ cells. There was a significant increase in the frequency of CD45$^+$Gr-1$^+$ (neutrophils) cells in CM group compared with AB alone 2 days post injury (Fig. 4E), while there was a lower frequency of CD45$^+$F4/80$^+$ cells (macrophages) compared with naïve corneas. The pattern of Gr-1$^+$ infiltration was similar to expression pattern of CXCL1 in cornea. These results are in agreement with the literature that showed that neutrophils can be found in central cornea as soon as 8 hours post injury.[43]

Because neutrophil infiltration peaked 2 days post injury, we measured MPO activity at the same time point, because MPO is the most abundant protein found in neutrophils. Our results, presented in Figure 4G, demonstrate that significantly higher MPO activity than control was seen in CM and AB groups, and MPO activity in CM was higher than AB. Myeloperoxidase activity in naïve control corneas was minimal, confirming the immunohistochemistry and flow cytometry results.

These results indicated that combining dry eye with AB worsens the severity of AB by increasing neutrophil infiltration and activity.

Discussion

Eye injuries can be very costly. In a 10-year review of eye injuries in the United States Army, Navy, and Air Force, Buckingham and colleagues[44,45] showed that the average military eye injury misfortune results in 4.7 to 6.1 days lost from work and has a cost ranging from $4222 to $9724. They also estimated that there was an underreporting of eye trauma data by at least 250%. Another underestimated factor is the cost for ambulatory visits, which is estimated to vary from $8.9 million to $14 million among the Army, Navy, and Air Force.[44] Therapeutic strategies for ocular surface chemical injuries have attempted to favorably modify one or more aspects of this process, during the acute phase. The visual outcomes from these injuries still remain poor in large part due to inadequate control of inflammatory and proteolytic components of the wound healing response.[46–48]

Dry eye can contribute to the severity of chemical and thermal injuries to the cornea, either during the initial healing phase following the burn or during the late phases. Dry eye can worsen the injury through a variety of events: reduced tear clearance and wash out, decrease provision of growth factors, and decrease corneal sensation and corneal exposure. Having all this in mind, we created a combined model where experimental dry eye is induced immediately after creation of AB and anesthetic recovery. We found that inhibition of tear production and exposure to desiccating environment markedly worsened corneal inflammation and matrix degradation, leading to perforation in nearly 40% of eyes. This was accompanied by increased production of IL-1β, IL-6, and MMPs mRNA transcripts as well as increased MMP-9 activity and MMP-1, -3, -13, and -9 immunoreactivity in corneal epithelium and increased frequency and function of neutrophils.

We observed that perforated corneas in the CM group showed detached epithelium, disrupted Bowman layer, and stromal ulceration. Although the basement membrane is not directly subjected to alkaline agents placed on the surface of the eye, its degradation by MMPs (collagenases and gelatinases) secreted by damaged or infiltrating cells contributes to the pathogenic ulceration and perforation of the stroma.[49] Stromal ulceration did not develop following alkali injury, in a

Investigative Ophthalmology & Visual Science

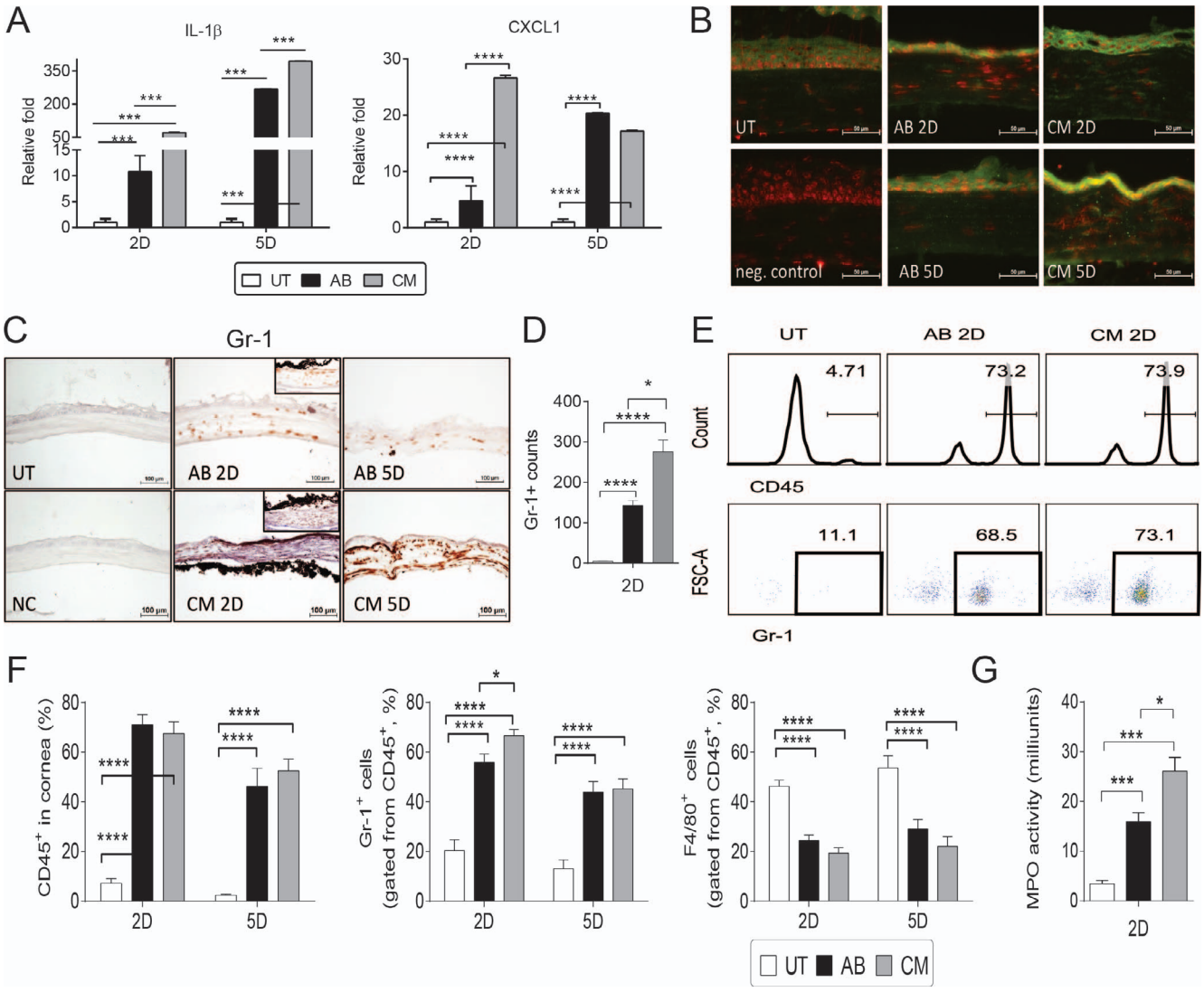

Figure 4. Increased neutrophil infiltration in CM groups. **(A)** Relative fold of expression of IL-1β and CXCL1 in whole corneas subjected to AB, or CM (AB + dry eye). *Bar graphs* show means ± SEM of one representative experiment with five samples per group/time point (experiment was repeated twice with similar results). $^{*}P < 0.05$, $^{**}P < 0.01$, $^{***}P < 0.001$, $^{****}P < 0.0001$. **(B)** Representative merged digital images of corneas cryosections immunostained for IL-1β (in *green*) with propidium iodide nuclei counterstaining (*red*) in corneas subjected to AB or CM. *Scale bars*: 50 μm. **(C)** Representative pictures of Gr-1$^+$ cells (*red*) of central cornea cryosections among the AB, CM, and control groups used to generate the *bar graph* showing counts in **(D)**. *Insets* are representative pictures of limbal area. **(D)** *Bar graphs* (mean ± SEM) of Gr-1$^+$ cell counts in whole cornea/groups. **(E)** Representative histogram (*top panel*) and dot plot (*bottom panel*) of CD45$^+$ and Gr-1$^+$ cells evaluated by flow cytometry. Numbers in the *squares* indicate percentage of positive cells. **(F)** *Bar graphs* (mean ± SEM) of frequency of CD45$^+$ and CD45$^+$Gr-1$^+$ and CD45$^+$F4/80$^+$ cells quantified by flow cytometry in whole-cornea, single-cell suspension. **(G)** Myeloperoxidase activity in whole-corneas lysates 2 days after injury in untreated, AB and CM groups (mean ± SEM). $^{*}P < 0.05$, $^{***}P < 0.001$, $^{****}P < 0.0001$. FSC-A, forward side scatter area.

standardized AB rabbit model using sodium hydroxide concentrations equal to or below 1N.[50] Healing after AB is characterized by extended inflammatory cell infiltration of the stroma, persistent epithelial defect, and degradation of the basement membrane and corneal neovascularization in late phases. In tissue sections from humans, different cell types can produce MMPs: neutrophils, stromal fibroblasts, and epithelial cells. It is important to note, however, that the cellular sources of collagenase appear to be somewhat species-dependent.[51] Studies in animal models of chemical or thermal injury revealed that there are very few fibroblasts in newly ulcerating corneas, due to cell death from the initiating agent. In the AB cornea, the epithelium surrounding the wound has long been thought to participate in stromal destruction.

We observed a significant increase in MMPs-1, -8, and -9 mRNA levels in the CM group compared with AB and DS. The activation of p38 MAPK alone has been shown to induce expression of MMP-1 and -3 in an activator protein 1 independent manner by stabilizing the corresponding mRNAs in human skin fibroblasts.[52] We have previously reported that DS upregulates MMPs, in particular MMP-3, and MMP-9 transcripts in the corneal epithelium.[19] The precise regulatory mechanisms inducing MMP production in wound healing have not yet been fully elucidated despite extensive investigations, but are thought to be stimulated by cytokines and growth factors, and cell–matrix or cell–cell interactions. During the repair period of cornea remodeling, the rate of collagen turnover is much higher than it is in the normal cornea,[51] suggesting the involvement of MMPs in the remodeling

Investigative Ophthalmology & Visual Science

process. In a rabbit model of superficial or penetrating injury to the stroma, increased expression of gelatinase (MMP-2), collagenases (MMP-1 and -13), and stromelysins MMP-3 was found.[24]

We found a significant increase in MMP-9 (both RNA and protein level, including activity) in corneas subjected to the combined model, peaking at 2 days post injury. Matrix metalloproteinase–9 has been implicated in both favoring and decreasing re-epithelization: MMP-9KO has been shown to accelerate healing of corneal wounds[37] while delaying re-epithelization in large cutaneous wound.[53,54] In human cornea wounds, MMP-9 is expressed in basal epithelial cells at the leading edge of the migrating epithelial front closing the corneal wound.[36] We have previously reported that human dry eye and experimental desiccating stress stimulates production of MMP-9, as well as other MMPs by the ocular surface epithelia.[19,55–57] MMP-9 was found to degrade the tight-junction protein occludin and to decrease apical epithelial barrier function in the cornea.[55] Matrix metalloproteinase–9 in human tears has also been found to increase in a variety of ocular surface diseases, including sterile corneal ulceration.[26,58–61] In a group of dry-eye patients, we observed a strong positive correlation between tear MMP-9 activity and severity of corneal epithelial disease. Tear MMP-9 activity levels also correlated positively with reduced contrast visual acuity.[21] The significant increase in MMP-9 in the combined model (~100-fold) compared with AB alone may suggest that MMP-9 could be delaying wound healing and facilitating cornea melting. Increased expression of MMP-9 and gelatinase activity has been reported in melted corneas from severe primary Sjögren Syndrome patients.[12] Interestingly, other MMPs were also present in these melted specimens, (intense MMP-1 and -7, and moderate MMP-3 and -8 immunoreactivity was noted).[12] The concentrations of IL-1β, IL-6, and MMP-8 and -9 were significantly upregulated in the tear fluid of the ulcer patients, corroborating our findings.[62]

Neutrophils are the first inflammatory cell responders to migrate toward the site of inflammation. Our results showed a significant influx of polymorphonuclears (PMNs) in the CM group, which coincides with a significant increase in CXCL1 in cornea. During the acute phase in corneal AB, the PMNs began to infiltrate the stroma, exerting their phagocytic functions to clear cellular debris, but at the same time, neutrophils release their proteolytic contents, including MMPs-1, -8, and -9[39] that may cause collateral damage. They enter the cornea from the limbus and move centrally in the superficial stroma somewhat behind the regenerating epithelium.[63] Collagenase breakdown products have been shown to be chemotactic for PMN.[64] Strategies developed to decrease neutrophil infiltration have been shown to improve wound healing following corneal alkali injury.[65,66] Neutrophil depleted C57BL/6 subjected to AB healed faster than nondepleted controls, demonstrating bystander damage to host tissue by PMN.[38]

Taken together our results showed that the stroma ulceration following AB is not simply the passive breakdown of alkali denatured collagen and proteoglycans, is a complex process involving interactions between different cell types, regulation of collagenases, cytokines, and growth factors. Moreover, they show that alkali injury in the context of a dry ocular surface dramatically exacerbates the inflammatory response and increases the rate of corneal perforation. This combined model is therefore more severe than regular AB and can be used to study severe devastating ocular injuries and facial burns that reach the eye, ocular injuries secondary to warfare agents and the effects of prolonged stay in environmental controlled low humidity intensive care unit on disease severity.

Acknowledgments

The authors thank Joel M. Sederstrom for his expert assistance with flow cytometry experiments and Mahira Zaheer and Kevin Tesareski for technical assistance.

Presented in part as abstracts at the annual meeting of the Association for Research in Vision and Ophthalmology, 2010, 2013, and 2014.

Supported by grants from W81XWH-12-1-0616 (CSDP; Department of Defense, Fort Detrick, MD, USA), National Institutes of Health (NIH) Training Grant T32-AI053831 (FB; Bethesda, MD, USA), National Eye Institute/NIH Core Grant EY-002520, Research to Prevent Blindness (New York, NY, USA), NIH funding to Cytometry and Cell Sorting Core at Baylor College of Medicine (NIAID P30AI036211, NCI P30CA125123, and NCRR S10RR024574), The Oshman Foundation (Houston, TX, USA), William Stamps Farish Fund (Houston, TX, USA), and The Hamill Foundation (Houston, TX, USA).

Disclosure: **F. Bian**, None; **F.S.A. Pelegrino**, None; **S.C. Pflugfelder**, None; **E.A. Volpe**, None; **D.-Q. Li**, None; **C.S. de Paiva**, None

References

1. Ward DL, Gorie C. Occupational eye injuries in soldiers. *J Occup Med*. 1991;33:646–650.
2. Lau JJ, Thach AB, Burden JH, Ward TP, Hshieh PB, Hollifield RD. Eye injuries in the U.S. Armed Forces. *Mil Med*. 2000;165:683–686.
3. Ari AB. Eye injuries on the battlefields of Iraq and Afghanistan: public health implications. *Optometry*. 2006;77:329–339.
4. Buglisi JA, Knoop KJ, Levsky ME, Euwema M. Experience with bandage contact lenses for the treatment of corneal abrasions in a combat environment. *Mil Med*. 2007;172:411–413.
5. Seet B, Wong TY. Military laser weapons: current controversies. *Ophthalmic Epidemiol*. 2001;8:215–226.
6. Wong TY, Seet MB, Ang CL. Eye injuries in twentieth century warfare: a historical perspective. *Surv Ophthalmol*. 1997;41:433–459.
7. Safarinejad MR, Moosavi SA, Montazeri B. Ocular injuries caused by mustard gas: diagnosis, treatment, and medical defense. *Mil Med*. 2001;166:67–70.
8. Kehe K, Thiermann H, Balszuweit F, Eyer F, Steinritz D, Zilker T. Acute effects of sulfur mustard injury—Munich experiences. *Toxicology*. 2009;263:3–8.
9. Nagase H, Woessner JF Jr. Matrix metalloproteinases. *J Biol Chem*. 1999;274:21491–21494.
10. Johnson LL, Dyer R, Hupe DJ. Matrix metalloproteinases. *Curr Opin Chem Biol*. 1998;2:466–471.
11. Visse R, Nagase H. Matrix metalloproteinases and tissue inhibitors of metalloproteinases: structure, function, and biochemistry. *Circ Res*. 2003;92:827–839.
12. Brejchova K, Liskova P, Hrdlickova E, Filipec M, Jirsova K. Matrix metalloproteinases in recurrent corneal melting associated with primary Sjörgen's syndrome. *Mol Vis*. 2009;15:2364–2372.
13. Alex A, Edwards A, Hays JD, et al. Factors predicting the ocular surface response to desiccating environmental stress. *Invest Ophthalmol Vis Sci*. 2013;54:3325–3332.
14. Wolkoff P, Kjaergaard SK. The dichotomy of relative humidity on indoor air quality. *Environ Int*. 2007;33:850–857.
15. Wolkoff P. "Healthy" eye in office-like environments. *Environ Int*. 2008;34:1204–1214.
16. Takahashi H, Igarashi T, Fujimoto C, Ozaki N, Ishizaki M. Immunohistochemical observation of amniotic membrane patching on a corneal alkali burn in vivo. *Jpn J Ophthalmol*. 2007;51:3–9.

17. de Paiva CS, Chotikavanich S, Pangelinan SB, et al. IL-17 disrupts corneal barrier following desiccating stress. *Mucosal Immunol*. 2009;2:243–253.
18. Yoeruek E, Ziemssen F, Henke-Fahle S, et al. Safety, penetration and efficacy of topically applied bevacizumab: evaluation of eyedrops in corneal neovascularization after chemical burn. *Acta Ophthalmol*. 2008;86:322–328.
19. Corrales RM, Stern ME, de Paiva CS, Welch J, Li DQ, Pflugfelder SC. Desiccating stress stimulates expression of matrix metalloproteinases by the corneal epithelium. *Invest Ophthalmol Vis Sci*. 2006;47:3293–3302.
20. Luo L, Li DQ, Doshi A, Farley W, Corrales RM, Pflugfelder SC. Experimental dry eye stimulates production of inflammatory cytokines and MMP-9 and activates MAPK signaling pathways on the ocular surface. *Invest Ophthalmol Vis Sci*. 2004;45:4293–4301.
21. Chotikavanich S, de Paiva CS, Li de Q, et al. Production and activity of matrix metalloproteinase-9 on the ocular surface increase in dysfunctional tear syndrome. *Invest Ophthalmol Vis Sci*. 2009;50:3203–3209.
22. Li DQ, Lokeshwar BL, Solomon A, Monroy D, Ji Z, Pflugfelder SC. Regulation of MMP-9 production by human corneal epithelial cells. *Exp Eye Res*. 2001;73:449–459.
23. Sobrin L, Liu Z, Monroy DC, et al. Regulation of MMP-9 activity in human tear fluid and corneal epithelial culture supernatant. *Invest Ophthalmol Vis Sci*. 2000;41:1703–1709.
24. Herretes S, Suwan-Apichon O, Pirouzmanesh A, et al. Use of topical human amniotic fluid in the treatment of acute ocular alkali injuries in mice. *Am J Ophthalmol*. 2006;142:271–278.
25. Sosne G, Christopherson PL, Barrett RP, Fridman R. Thymosin-beta4 modulates corneal matrix metalloproteinase levels and polymorphonuclear cell infiltration after alkali injury. *Invest Ophthalmol Vis Sci*. 2005;46:2388–2395.
26. Afonso AA, Sobrin L, Monroy DC, Selzer M, Lokeshwar B, Pflugfelder SC. Tear fluid gelatinase B activity correlates with IL-1alpha concentration and fluorescein clearance in ocular rosacea. *Invest Ophthalmol Vis Sci*. 1999;40:2506–2512.
27. de Paiva CS, Corrales RM, Villarreal AL, et al. Corticosteroid and doxycycline suppress MMP-9 and inflammatory cytokine expression, MAPK activation in the corneal epithelium in experimental dry eye. *Exp Eye Res*. 2006;83:526–535.
28. Lavigne MC, Thakker P, Gunn J, et al. Human bronchial epithelial cells express and secrete MMP-12. *Biochem Biophys Res Commun*. 2004;324:534–546.
29. Iwanami H, Ishizaki M, Fukuda Y, Takahashi H. Expression of matrix metalloproteinases (MMP)-12 by myofibroblasts during alkali-burned corneal wound healing. *Curr Eye Res*. 2009;34:207–214.
30. Chan MF, Li J, Bertrand A, et al. Protective effects of matrix metalloproteinase-12 following corneal injury. *J Cell Sci*. 2013;126:3948–3960.
31. Ye HQ, Maeda M, Yu FX, Azar DT. Differential expression of MT1-MMP (MMP-14) and collagenase III (MMP-13) genes in normal and wounded rat corneas. *Invest Ophthalmol Vis Sci*. 2000;41:2894–2899.
32. Dumin JA, Dickeson SK, Stricker TP, et al. Pro-collagenase-1 (matrix metalloproteinase-1) binds the alpha(2)beta(1) integrin upon release from keratinocytes migrating on type I collagen. *J Biol Chem*. 2001;276:29368–29374.
33. Johnson JL, Dwivedi A, Somerville M, George SJ, Newby AC. Matrix metalloproteinase (MMP)-3 activates MMP-9 mediated vascular smooth muscle cell migration and neointima formation in mice. *Arterioscler Thromb Vasc Biol*. 2011;31:e35–e44.
34. Fini ME, Girard MT, Matsubara M. Collagenolytic/gelatinolytic enzymes in corneal wound healing. *Acta Ophthalmol Suppl*. 1992;26–33.
35. Matsubara M, Girard MT, Kublin CL, Cintron C, Fini ME. Differential roles for two gelatinolytic enzymes of the matrix metalloproteinase family in the remodelling cornea. *Dev Biol*. 1991;147:425–439.
36. Matsubara M, Zieske JD, Fini ME. Mechanism of basement membrane dissolution preceding corneal ulceration. *Invest Ophthalmol Vis Sci*. 1991;32:3221–3237.
37. Mohan R, Chintala SK, Jung JC, et al. Matrix metalloproteinase gelatinase B (MMP-9) coordinates and effects epithelial regeneration. *J Biol Chem*. 2002;277:2065–2072.
38. Ueno M, Lyons BL, Burzenski LM, et al. Accelerated wound healing of alkali-burned corneas in MRL mice is associated with a reduced inflammatory signature. *Invest Ophthalmol Vis Sci*. 2005;46:4097–4106.
39. Tiku K, Tiku ML, Skosey JL. Interleukin 1 production by human polymorphonuclear neutrophils. *J Immunol*. 1986;136:3677–3685.
40. Wilson SE, He Y-G, Lloyd SA. EGF receptor, basic FGF, TGF-beta-1, and IL-1 alpha mRNA in human corneal epithelial cells and stromal fibroblasts. *Invest Ophthalmol Vis Sci*. 1992;33:1756–1765.
41. Li Q, Fukuda K, Lu Y, et al. Enhancement by neutrophils of collagen degradation by corneal fibroblasts. *J Leukoc Biol*. 2003;74:412–419.
42. De FK, Dudeck A, Hasenberg M, et al. Mast cell and macrophage chemokines CXCL1/CXCL2 control the early stage of neutrophil recruitment during tissue inflammation. *Blood*. 2013;121:4930–4937.
43. Hanlon SD, Smith CW, Sauter MN, Burns AR. Integrin-dependent neutrophil migration in the injured mouse cornea. *Exp Eye Res*. 2014;120:61–70.
44. Buckingham RS, Whitwell KJ, Lee RB. Cost analysis of military eye injuries in fiscal years 1988–1998. *Mil Med*. 2005;170:196–200.
45. Buckingham RS, Whitwell KJ, Lee RB. Department of defense eye injuries from fiscal year 1988-1998. *Optometry*. 2001;72:653–660.
46. Solomon A, Rosenblatt M, Li D, et al. Doxycycline inhibition of interleukin-1 in the corneal epithelium. *Am J Ophthalmol*. 2000;130:688.
47. Fini ME, Cui TY, Mouldovan A, Grobelny D, Galardy RE, Fisher SJ. An inhibitor of the matrix metalloproteinase synthesized by rabbit corneal epithelium. *Invest Ophthalmol Vis Sci*. 1991;32:2997–3001.
48. Kato T, Saika S, Ohnishi Y. Effects of the matrix metalloproteinase inhibitor GM6001 on the destruction and alteration of epithelial basement membrane during the healing of post-alkali burn in rabbit cornea. *Jpn J Ophthalmol*. 2006;50:90–95.
49. Saika S, Ikeda K, Yamanaka O, et al. Therapeutic effects of adenoviral gene transfer of bone morphogenic protein-7 on a corneal alkali injury model in mice. *Lab Invest*. 2005;85:474–486.
50. Ormerod LD, Abelson MB, Kenyon KR. Standard models of corneal injury using alkali-immersed filter discs. *Invest Ophthalmol Vis Sci*. 1989;30:2148–2153.
51. Fini ME, Cook JR, Mohan R. Proteolytic mechanisms in corneal ulceration and repair. *Arch Dermatol Res*. 1998;290(suppl):S12–S23.
52. Capoulade C, Mir LM, Carlier K, et al. Apoptosis of tumoral and nontumoral lymphoid cells is induced by both mdm2 and p53 antisense oligodeoxynucleotides. *Blood*. 2001;97:1043–1049.
53. Reiss MJ, Han YP, Garcia E, Goldberg M, Yu H, Garner WL. Matrix metalloproteinase-9 delays wound healing in a murine wound model. *Surgery*. 2010;147:295–302.

Investigative Ophthalmology & Visual Science

54. Hattori N, Mochizuki S, Kishi K, et al. MMP-13 plays a role in keratinocyte migration, angiogenesis, and contraction in mouse skin wound healing. *Am J Pathol*. 2009;175:533–546.
55. Pflugfelder SC, Farley W, Luo L, et al. Matrix metalloproteinase-9 knockout confers resistance to corneal epithelial barrier disruption in experimental dry eye. *Am J Pathol*. 2005;166:61–71.
56. de Paiva CS, Corrales RM, Villarreal AL, et al. Corticosteroid and doxycycline suppress MMP-9 and inflammatory cytokine expression, MAPK activation in the corneal epithelium in experimental dry eye. *Exp Eye Res*. 2006;83:526–535.
57. Luo L, Li DQ, Corrales RM, Pflugfelder SC. Hyperosmolar saline is a proinflammatory stress on the mouse ocular surface. *Eye Contact Lens*. 2005;31:186–193.
58. Leonardi A, Brun P, Abatangelo G, Plebani M, Secchi AG. Tear levels and activity of matrix metalloproteinase (MMP)-1 and MMP-9 in vernal keratoconjunctivitis. *Invest Ophthalmol Vis Sci*. 2003;44:3052–3058.
59. Sakimoto T, Shoji J, Sawa M. Active form of gelatinases in tear fluid in patients with corneal ulcer or ocular burn. *Jpn J Ophthalmol*. 2003;47:423–426.
60. Gabison EE, Chastang P, Menashi S, et al. Late corneal perforation after photorefractive keratectomy associated with topical diclofenac: involvement of matrix metalloproteinases. *Ophthalmology*. 2003;110:1626–1631.
61. Reviglio VE, Rana TS, Li QJ, Ashraf MF, Daly MK, O'Brien TP. Effects of topical nonsteroidal antiinflammatory drugs on the expression of matrix metalloproteinases in the cornea. *J Cataract Refract Surg*. 2003;29:989–997.
62. Sakimoto T, Ohnishi T, Ishimori A. Simultaneous study of matrix metalloproteinases, proinflammatory cytokines, and soluble cytokine receptors in the tears of noninfectious corneal ulcer patients. *Graefes Arch Clin Exp Ophthalmol*. 2014;252:1451–1456.
63. Li ZY, Wallace RN, Streeten BW, Kuntz BL, Dark AJ. Elastic fiber components and protease inhibitors in pingucula. *Invest Ophthalmol Vis Sci*. 1991;32:1573–1585.
64. Seedor JA, Perry HD, McNamara TF, Golub LM, Buxton DF, Guthrie DS. Systemic tetracycline treatment of alkali-induced corneal ulceration in rabbits. *Arch Ophthalmol*. 1987;105:268–271.
65. Kenyon KR, Berman M, Rose J, Gage J. Prevention of stromal ulceration in the alkali-burned rabbit cornea by glued-on contact lens. Evidence for the role of polymorphonuclear leukocytes in collagen degradation. *Invest Ophthalmol Vis Sci*. 1979;18:570–587.
66. Foster CS, Zelt RP, Mai-Phan T, Kenyon KR. Immunosuppression and selective inflammatory cell depletion. Studies on a guinea pig model of corneal ulceration after ocular alkali burning. *Arch Ophthalmol*. 1982;100:1820–1824.

Investigative Ophthalmology & Visual Science